Supplementary Information: Cavity-mediated electron-photon superconductivity

Frank Schlawin[1], Andrea Cavalleri[1,2] and Dieter Jaksch[1]
[1] *Clarendon Laboratory, University of Oxford, Parks Road, Oxford OX1 3PU, United Kingdom* and*
[2] *Max Planck Institute for the Structure and Dynamics of Matter, Luruper Chaussee 149, 22761 Hamburg, Germany*

I. THE MODEL

A. Cavity field quantisation

The setup is sketched in Fig. 1(a) of the main text. We model the cavity as perfectly reflecting mirrors at $z = 0$ and L, with the 2D electron gas at the centre at $z_0 = L/2$. The tangential component of the electric field and the normal component of the magnetic fields must vanish at the mirrors' position. In addition, we impose periodic boundary conditions in the xy-plane. Given an electronic system filling the xy-plane with a spacing a between the lattice sites, the size of the cavity in the plane is $L_x L_y = Na^2$. For the mean field, we shall consider the thermodynamic limit $N \to \infty$.

To derive expressions for the cavity field, we follow the derivation in [1]. The boundary conditions are satisfied by the vector potential of the form

$$\vec{A'} = \sum_{\vec{q}} \sqrt{\frac{\hbar}{\epsilon\epsilon_0 V\omega_q}} e^{i(q_x x+q_y y)} \begin{pmatrix} (b_x - b_x^\dagger) i \sin(\frac{\pi z}{L}) \\ (b_y - b_y^\dagger) i \sin(\frac{\pi z}{L}) \\ (b_z + b_z^\dagger) \cos(\frac{\pi z}{L}) \end{pmatrix}, \tag{S1}$$

where b_n denotes the field amplitude in the n-th direction, ϵ the filling material dielectric constant, and ϵ_0 the vacuum dielectric constant. Transversality imposes $\vec{q}\cdot\vec{A} = 0$, such that the b_i are not linearly independent. Therefore, we write $\vec{q} = |q|(\sin\theta\cos\phi, \sin\theta\sin\phi, \cos\theta)$, and rotate to a new basis, in which the z-component is parallel to $\vec{q}$, with the rotation matrix

$$O^q = \begin{pmatrix} \cos\theta\cos\phi & \cos\theta\sin\phi & -\sin\theta \\ -\sin\phi & \cos\phi & 0 \\ \sin\theta\cos\phi & \sin\theta\sin\phi & \cos\theta \end{pmatrix}. \tag{S2}$$

The new eigenmodes are then given by $\vec{u}_{\vec{q}s} = \sum_i \hat{e}_i O^q_{si} u_{\vec{q}i}$, and we obtain the two transverse field modes

$$\vec{A} = i\sum_{\vec{q},s} \sqrt{\frac{\hbar}{\epsilon\epsilon_0 V\omega_q}} \hat{e}_{\vec{q},s} e^{i(q_x x+q_y y)} \left(a_{\vec{q},s} + a^\dagger_{-\vec{q},s}\right), \tag{S3}$$

with the polarisation vector

$$\hat{e}_{\vec{q},1} = \frac{\vec{q}}{|\vec{q}|}, \tag{S4}$$

which is called the transverse electric mode. Here, we have set $\pi z_0/L = \pi/2$, *i.e.* the electron system is placed at the maximum of the cavity field.

The second polarisation is given by

$$\hat{e}_{\vec{q},2} = \hat{e}_{\vec{q},1} \times \hat{e}_z \tag{S5}$$

and is called the transverse magnetic mode. The z-component of the field can be neglected, and we obtain the vector potential

$$\vec{A}(\vec{r}) = i\sum_{\vec{q},s} \sqrt{\frac{\hbar}{\epsilon\epsilon_0 V\omega_q}} e^{i(q_x x+q_y y)} \hat{e}_{\vec{q},s} \left(a_{\vec{q},s} + a^\dagger_{-\vec{q},s}\right). \tag{S6}$$

Note that the transverse magnetic mode also has a gapless mode with $k_z = 0$, which is however polarised along the z-direction [2], and does not couple to the electronic system in the present setup.

In principle, this setup also features higher dispersion bands starting at frequencies $(2n+1)\omega_0$, where n is a natural number (even multiples of ω_0 have a node at the position of the electron gas, and hence do not couple to it). For $\omega_0 = 2\pi\times 5$ THz, these higher dispersion bands are in the optical regime, and one cannot expect a THz cavity to still confine the light at such high frequencies, so we do not take these into account.

B. Coupling to electron field

The paramagnetic Hamiltonian couples the cavity field to the current operator of the electron system, and reads in real space

$$H_{int} = \sum_{\vec{n}} \vec{j}(\vec{r}_{\vec{n}}) \cdot \vec{A}((\vec{r}_{\vec{n}+1} - \vec{r}_{\vec{n}})/2), \tag{S7}$$

where $\vec{n}$ denotes the summation over the lattice sites. In a rectangular lattice with nearest-neighbour hopping, the current operator is given by

$$\vec{j}_n = \frac{iaet}{\hbar} \sum_{i=x,y} \sum_{\vec{n},\sigma} \hat{e}_i \left(c^\dagger_{\vec{n}+1_i\sigma} c_{\vec{n},\sigma} - c^\dagger_{\vec{n},\sigma} c_{\vec{n}+1_i\sigma}\right), \tag{S8}$$

where $\vec{n}+1_x = (n_x+1, n_y)$ and $\vec{n}+1_y = (n_x, n_y+1)$. Using the form of the vector potential (S6), the interaction Hamiltonian in k-space then reads

$$H_{int} = \sum_{\vec{k},\sigma,\vec{q},s} \frac{g^{(\vec{q})}_{\vec{k},s}}{\sqrt{N}} \left(a_{\vec{q},s} + a^\dagger_{-\vec{q},s}\right) c^\dagger_{\vec{k}+\vec{q},\sigma} c_{\vec{k},\sigma}, \tag{S9}$$

with

$$g^{(\vec{q})}_{\vec{k},1} = i\tilde{g}_0 \frac{\hat{e}_{\vec{q},1,x}\sin[(k_x+q_x/2)] + \hat{e}_{\vec{q},1,y}\sin[(k_y+q_y/2)]}{\left(1+\left(\frac{c\vec{q}}{\omega_0}\right)^2\right)^{1/4}}, \tag{S10}$$

* frank.schlawin@physics.ox.ac.uk

and

$$g^{(\vec{q})}_{\vec{k},2} = i\tilde{g}_0 \frac{\hat{e}_{\vec{q},2,x}\sin[(k_x+q_x/2)] + \hat{e}_{\vec{q},2,y}\sin[(k_y+q_y/2)]}{\left(1+\left(\frac{c\vec{q}}{\omega_0}\right)^2\right)^{1/4}}, \tag{S11}$$

where in our setup

$$\tilde{g}_0 = t\sqrt{\frac{4\alpha}{\sqrt{\epsilon}}}, \tag{S12}$$

$$\simeq 0.1t. \tag{S13}$$

Here, $\alpha \simeq 1/137$ denotes the fine structure constant, and we used $\epsilon = 13$ for GaAs (see table I). This coefficient is similar to the one obtained in [3] for the coupling of cyclotron transitions to a cavity field. The coefficients obey the symmetry $g^{(-\vec{q})}_{-\vec{k},s} = g^{(\vec{q})}_{\vec{k},s}$ and $g^{(-\vec{q})}_{\vec{k},s} \simeq g^{(\vec{q})*}_{\vec{k},s}$.

This is the cavity coupling for a half-wavelength cavity with $\omega_0 = c\pi/L_z$. In the case of a nanoplasmonic cavity, the field is further enhanced below the free-space limit. For instance, in Ref. [4], the cavity volume is estimated to be $V = 2.5\times10^{-5}\times(\lambda_0/2\sqrt{\epsilon})^3$, where λ_0 is the vacuum cavity wavelength. It is this further compression of the cavity field that enables the experiments to reach the ultrastrong coupling regime, where the coupling becomes comparable to the cavity frequency. To describe this situation phenomenologically (*i.e.* without ab initio simulation of the cavity field), we rescale $\tilde{g}_0$ by the reduction of the mode volume below the λ^3-limit,

$$g_0 = \frac{\tilde{g}_0}{\sqrt{A}}, \tag{S14}$$

where we define the reduction of the cavity below the far field limit A.

II. PARAMETER VALUES FOR GAAS HETEROSTRUCTURES

Electron band mass	$m^* = 0.07\, m_e$
Lattice constant	$a = 5.6$ Å
Dielectric constant	$\epsilon = 13$
Electron density	$n_e = 3.6\times10^{11}$ cm^{-2}
Cavity frequency	$\omega_0 = 2\pi\times 5$ THz

TABLE I. Parameters of GaAs used for the estimation of the critical temperature.

The parameters are obtained from reported values in [4, 7–9], and are given in table I. From these, we calculate the transfer integral

$$t = \frac{\hbar^2}{2m^*a^2}, \tag{S15}$$

and the Fermi wavevector (which we measure in units of the lattice constant a)

$$k_f a = \sqrt{2\pi n_e}a \simeq 0.084. \tag{S16}$$

For low filling ratios, the electron dispersion is approximately quadratic,

$$\epsilon_k \approx ta^2\left(k_x^2+k_y^2\right) - \tilde{\mu} \tag{S17}$$

$$= \frac{\hbar^2}{2m^*}\left(k_x^2+k_y^2\right) - \tilde{\mu}, \tag{S18}$$

with $\tilde{\mu} = 4t+\mu$. We use Eqs. (S16) and (S18) to relate the electron density to the chemical potential,

$$n_e = \frac{m^*}{\pi\hbar^2}(4t+\mu). \tag{S19}$$

The speed of light in GaAs in given by

$$c = c_0/\sqrt{\epsilon}, \tag{S20}$$

where $c_0 = 3\times10^8$ m/s is the vacuum speed of light.

In the case of a two-dimensional electron gas GaAs heterostructures, the screened Coulomb repulsion is given by [9]

$$V_C(\vec{k}) = \frac{1}{2\epsilon\epsilon_0 Na^2}\frac{e^2}{|\vec{k}|+k_{TF}}, \tag{S21}$$

with the vacuum permittivity ϵ_0 and the inverse screening length $k_{TF} = me^2/(2\pi\epsilon\epsilon_0\hbar^2)$, we obtain an approximate Hubbard-U (for $\vec{k}=0$), $U \simeq 0.25t$.

III. WOLF-SCHRIEFFER TRANSFORMATION

To obtain the effective cavity-mediated interaction, we eliminate the interaction Hamiltonian (S9) by a Wolf-Schrieffer transformation, *i.e.* we rotate to a new frame with Hamiltonian

$$H' \equiv e^S\left(H_0+H_f+H_{int}\right)e^{-S} \tag{S22}$$

$$= H_0+H_f+H_{int}+\left[S,H_0+H_f+H_{int}\right]$$

$$+\frac{1}{2}\left[S,\left[S,H_0+H_f\right]\right]+\ldots \tag{S23}$$

where we choose S, such that

$$\left[S,H_0+H_f\right] = -H_{int}, \tag{S24}$$

and thereby eliminate the coupling to the cavity to leading order. This is the case for

$$S = \sum_{\vec{k},\vec{q},\sigma,s}\frac{g^{(\vec{q})}_{\vec{k},s}}{\sqrt{N}}\left(x^{(s)}_{\vec{k},\vec{q}}a_{\vec{q},s} + y^{(s)}_{\vec{k},\vec{q}}a^\dagger_{-\vec{q},s}\right)c^\dagger_{\vec{k}+\vec{q},\sigma}c_{\vec{k},\sigma}, \tag{S25}$$

with

$$x^{(s)}_{\vec{k},\vec{q}} = -\frac{1}{\epsilon_{\vec{k}+\vec{q}}-\epsilon_{\vec{k}}-\hbar\omega_{\vec{q}}} \tag{S26}$$

and

$$y^{(s)}_{\vec{k},\vec{q}} = -\frac{1}{\epsilon_{\vec{k}+\vec{q}}-\epsilon_{\vec{k}}+\hbar\omega_{\vec{q}}}. \tag{S27}$$

From Eq. (S23), we then obtain

$$H_{\text{eff}} = \frac{1}{2N}\sum_{\vec{k},\vec{k}',\vec{q}}\sum_{\sigma,\sigma',s}\frac{2\hbar\omega_q g^{(\vec{q})}_{\vec{k},s} g^{(-\vec{q})}_{\vec{k}',s}}{(\epsilon_{\vec{k}+\vec{q}}-\epsilon_{\vec{k}})^2-(\hbar\omega_q)^2} c^\dagger_{\vec{k}+\vec{q},\sigma} c_{\vec{k},\sigma} c^\dagger_{\vec{k}'-\vec{q},\sigma'} c_{\vec{k}',\sigma'}. \tag{S28}$$

Keeping in mind that $\hbar\omega_q \gg |\epsilon_{\vec{k}} - \epsilon_{\vec{k}'}|$, we can always replace

$$\frac{2\hbar\omega_q}{(\epsilon_{\vec{k}+\vec{q}}-\epsilon_{\vec{k}})^2-(\hbar\omega_q)^2} \simeq -\frac{2}{\hbar\omega_{\vec{q}}}. \tag{S29}$$

A. Change of electron dispersion

In tracing out the photon field, one also obtains a renormalisation of the electronic band structure due to scattering processes, when $\vec{k}' = \vec{k} + \vec{q}$ and $\sigma' = \sigma$. We obtain

$$H_{\text{St}} = \sum_{\vec{k},\sigma} h_{\vec{k}} c^\dagger_{\vec{k}\sigma} c_{\vec{k}\sigma}, \tag{S30}$$

with

$$h_{\vec{k}} = -\frac{1}{N}\sum_{\vec{q},s}\frac{g^{(\vec{q})}_{\vec{k}-\vec{q},s} g^{(-\vec{q})}_{\vec{k},s}}{\hbar\omega_q} \tag{S31}$$

$$= -\frac{g_0^2}{N\hbar\omega_0}\left(\frac{\omega_0}{c}\right)^2 \sum_{\vec{q}}\frac{\sum_{i=x,y}\sin^2[(k_i a - q_i a/2)]}{(\omega_0/c)^2+q^2}. \tag{S32}$$

It can be estimated to be on the order of

$$h_{\vec{k}} \simeq -\pi V_0 k_f^2\left(\frac{a\omega_0}{c}\right)^2\int_0^{q_{\max}} dq\frac{q}{(\omega_0/c)^2+q^2} \tag{S33}$$

$$\simeq -\pi V_0 k_f^2\left(\frac{a\omega_0}{c}\right)^2 \log\left[1+\left(\frac{c}{\omega_0}q_{\max}\right)\right], \tag{S34}$$

where $q_{\max}$ denotes a cutoff frequency for the in-plane photon momenta supported by the cavity (see also section IV D). In the first line, we approximated the numerator of Eq. (S32) by $\sim 2k_f^2 a^2$. The additional factor 2π stems from the integration over the azimuthal angle. Using values appropriate for GaAs, we obtain $h_{\vec{k}} \sim 1.25\times10^{-8}A^{-1}$. Thus, even if the mode volume compression is as small as $A = 10^{-5}$, the change in the electron dispersion would on the order of 0.1 %. It can therefore be neglected.

B. The diamagnetic interaction

As shown theoretically in [3], and observed experimentally in [7], the diamagnetic interaction, which can be neglected in most cases of interest in the optical regime, can become relevant or even dominant at strong resonant coupling. The diamagnetic interaction Hamiltonian reads

$$H_{dia} = \sum_{\vec{k},\vec{q},\vec{q}',s,\sigma}\gamma_{\vec{k},\vec{q},\vec{q}'}\left(a_{\vec{q}'-\vec{q},s}+a^\dagger_{\vec{q}-\vec{q}',s}\right)\left(a_{\vec{q},s}+a^\dagger_{-\vec{q},s}\right)c^\dagger_{\vec{k}+\vec{q},\sigma}c_{\vec{k}\sigma}, \tag{S35}$$

where

$$\gamma_{\vec{k},\vec{q},\vec{q}'} = -\frac{t}{A}\left(\frac{ea}{\hbar}\right)^2\sqrt{\frac{\hbar}{\epsilon V\omega_q}}\sqrt{\frac{\hbar}{\epsilon V\omega_{q'}}}\hat{e}_{\vec{q},s}\cdot\hat{e}_{\vec{q},s}. \tag{S36}$$

The prefactor can be estimated as (see section IV D)

$$\left|\gamma_{\vec{k},\vec{q},\vec{q}'}\right| \sim \frac{t}{A}\frac{4\alpha}{\sqrt{\epsilon}}\left(\frac{a\omega_0}{c}\right)^2\log\left[1+\left(\frac{c}{\omega_0}q_{\max}\right)\right] \sim 10^{-8}\frac{t}{A}, \tag{S37}$$

and can only give rise to minimal changes of the electron self-energy. Again, it can be safely neglected, as long as the cavity is in its ground state.

IV. MEAN FIELD THEORY

A. The pair density wave

Considering only the attractive Amperean channel in the nesting wavevectors $\vec{Q} = k_0(\pm1,\pm1)$, the electronic Hamiltonian reads

$$H = \sum_{\vec{k},\sigma}\epsilon_{\vec{k}}c^\dagger_{\vec{k},\sigma}c_{\vec{k},\sigma} + \frac{1}{2N}\sum_{\vec{Q},\vec{p},\vec{p}'}\sum_{\sigma,\sigma'}V^{(\vec{Q})}_{\vec{p},\vec{p}'}c^\dagger_{\vec{Q}+\vec{p},\sigma}c_{\vec{Q}+\vec{p}',\sigma}c^\dagger_{\vec{Q}-\vec{p},\sigma'}c_{\vec{Q}-\vec{p}',\sigma'}. \tag{S38}$$

We define the order parameters

$$\Delta^{(\vec{Q})}_{\sigma,\sigma'}(\vec{p}) = \frac{1}{N}\sum_{\vec{p}'}V^{(\vec{Q})}_{\vec{p},\vec{p}'}\left\langle c_{\vec{Q}-\vec{p}',\sigma'}c_{\vec{Q}+\vec{p}',\sigma}\right\rangle, \tag{S39}$$

and arrive at the mean field Hamiltonian

$$H_{\text{MF}} = \frac{1}{2}\sum_{\vec{Q},\vec{p}}\begin{pmatrix}c^\dagger_{\vec{Q}+\vec{p},\uparrow} & c^\dagger_{\vec{Q}+\vec{p},\downarrow} & c_{\vec{Q}-\vec{p},\uparrow} & c_{\vec{Q}-\vec{p},\downarrow}\end{pmatrix}\begin{pmatrix}\epsilon_{\vec{Q}+\vec{p}} & 0 & \Delta^{(\vec{Q})}_{\uparrow\uparrow}(\vec{p}) & \Delta^{(\vec{Q})}_{\uparrow\downarrow}(\vec{p})\\ 0 & \epsilon_{\vec{Q}+\vec{p}} & \Delta^{(\vec{Q})}_{\downarrow\uparrow}(\vec{p}) & \Delta^{(\vec{Q})}_{\downarrow\downarrow}(\vec{p})\\ \Delta^{(\vec{Q})*}_{\uparrow\uparrow}(\vec{p}) & \Delta^{(\vec{Q})*}_{\downarrow\uparrow}(\vec{p}) & -\epsilon_{\vec{Q}-\vec{p}} & 0\\ \Delta^{(\vec{Q})*}_{\uparrow\downarrow}(\vec{p}) & \Delta^{(\vec{Q})*}_{\downarrow\downarrow}(\vec{p}) & 0 & -\epsilon_{\vec{Q}-\vec{p}}\end{pmatrix}\begin{pmatrix}c_{\vec{Q}+\vec{p},\uparrow}\\ c_{\vec{Q}+\vec{p},\downarrow}\\ c^\dagger_{\vec{Q}-\vec{p},\uparrow}\\ c^\dagger_{\vec{Q}-\vec{p},\downarrow}\end{pmatrix} + \sum_{\vec{Q},\vec{p}}\epsilon_{\vec{Q}-\vec{p}}. \tag{S40}$$

This representation contains singlet and triplet components. The dominating symmetry cannot be deduced in this form.

B. Single mean field

We consider only one order parameter, in which case the mean field Hamiltonian reduces to

$$H'_{\mathrm{MF}} = \sum_{\vec{Q},\vec{p}} \begin{pmatrix} c^\dagger_{\vec{Q}+\vec{p},\sigma} & c_{\vec{Q}-\vec{p},\sigma'} \end{pmatrix} \begin{pmatrix} \epsilon_{\vec{Q}+\vec{p}} & \Delta^{(\vec{Q})}_{\sigma\sigma'}(\vec{p}) \\ \Delta^{(\vec{Q})*}_{\sigma\sigma'}(\vec{p}) & -\epsilon_{\vec{Q}-\vec{p}} \end{pmatrix} \begin{pmatrix} c_{\vec{Q}+\vec{p},\sigma} \\ c_{\vec{Q}-\vec{p},\sigma'} \end{pmatrix}. \tag{S41}$$

It can be diagonalised straightforwardly, and we obtain

$$H'_{\mathrm{MF}} = \sum_{\vec{Q},\vec{p}} \begin{pmatrix} \gamma^\dagger_{\vec{Q}+\vec{p},\sigma} & \gamma_{\vec{Q}-\vec{p},\sigma'} \end{pmatrix} \begin{pmatrix} E_+ & 0 \\ 0 & E_- \end{pmatrix} \begin{pmatrix} \gamma_{\vec{Q}+\vec{p},\sigma} \\ \gamma^\dagger_{\vec{Q}-\vec{p},\sigma'} \end{pmatrix}, \tag{S42}$$

with $E_\pm = \frac{1}{2}(\epsilon_{\vec{Q}+\vec{p}} - \epsilon_{\vec{Q}-\vec{p}}) \pm \sqrt{(\epsilon_{\vec{Q}+\vec{p}} + \epsilon_{\vec{Q}-\vec{p}})^2/4 + |\Delta^{(\vec{Q})}(\vec{p})|^2}$. Note that in contrast to regular BCS theory, this Hamiltonian has no particle-hole symmetry, $E_- \neq -E_+$.

The gap equation reads

$$\Delta^{(\vec{Q})}_{\sigma,\sigma'}(\vec{p}) = -\frac{1}{N}\sum_{\vec{p}'} V^{(\vec{Q})}_{\vec{p},\vec{p}'} \left\langle c_{\vec{Q}-\vec{p}',\sigma'} c_{\vec{Q}+\vec{p}',\sigma} \right\rangle \tag{S43}$$

$$= -\frac{1}{N}\sum_{\vec{p}'} V^{(\vec{Q})}_{\vec{p},\vec{p}'} \frac{\Delta(\vec{p}')}{2\sqrt{\zeta^2_{\vec{p}'} + |\Delta(\vec{p}')|^2}} \left(f_{\vec{p}'} + f_{-\vec{p}'} - 1\right), \tag{S44}$$

where $f_{\vec{p}} = (\exp(E_+(\vec{p})/k_BT)+1)^{-1}$, and $\zeta_p = (\epsilon_{\vec{Q}+\vec{p}}+\epsilon_{\vec{Q}-\vec{p}})/2$. Due to the lack of particle-hole symmetry, the expression does not simplify to the usual gap equation, since

$$f_{-\vec{p}} = \frac{1}{e^{E_+(-\vec{p})/kBT}} = \frac{1}{e^{(E_+(\vec{p})-(\epsilon_{\vec{Q}+\vec{p}}-\epsilon_{\vec{Q}-\vec{p}}))/kBT}} \neq f_{\vec{p}}. \tag{S45}$$

Thus, in the continuous limit we obtain

$$\Delta^{(\vec{Q})}_{\sigma,\sigma'}(\vec{p}) = -\frac{|V_0|}{2(2\pi)^2}\int d^2p' \frac{1}{2} \frac{\cos(p_x+p'_x)a + \cos(p_y+p'_y)a - \cos 2Q_x a - \cos 2Q_y a}{(\omega_0/c)^2 + \left|\vec{p}' - \vec{p}\right|^2} \frac{\Delta^{(\vec{Q})}_{\sigma,\sigma'}(\vec{p}')}{\sqrt{\zeta^2_{\vec{p}'} + |\Delta_{\vec{p}'}|^2}} \left(f_{\vec{p}'} + f_{-\vec{p}'} - 1\right). \tag{S46}$$

As we will describe in the next section, the deviation from a conventional BCS theory are negligibly small; at least, when we are determining the critical temperature.

C. Critical temperature

We wish to switch the integration over the full Brillouin zone in Eq. (S46) into an integration along the Fermi surface, and one integration along the energy axis ζ. To find deviations from conventional BCS theory, we write

$$f_{\vec{p}'} + f_{-\vec{p}'} - 1 = \frac{1}{e^{(\zeta+\delta)/k_BT}+1} + \frac{1}{e^{(\zeta-\delta)/k_BT}+1} - 1, \tag{S47}$$

where δ denotes the deviation of the quasiparticle dispersion from ζ. Expanding around $\delta = 0$ (at the Fermi surface), we find

$$f_{\vec{p}'} + f_{-\vec{p}'} - 1 \simeq -\tanh\left(\frac{\zeta}{2k_BT}\right) + 2\left(\frac{\delta}{k_BT}\right)^2 \frac{\sinh^4(\zeta/(2k_BT))}{\sinh^3(\zeta/(k_BT))} + \dots \tag{S48}$$

Linearising Eq. (S46) near T_c, and switching the integration variables to an integration along the energy axis, and along the Fermi surface, we obtain the eigenvalue equation (5) of the main text. The energy integration yields for the first term in Eq. (S48) the well-known result

$$\int_0^{\hbar\omega_c} \frac{d\zeta}{\zeta} \tanh\left(\frac{\zeta}{2k_BT_c}\right) \simeq \ln\left(\frac{1.1.3\hbar\omega_c}{k_BT_c}\right), \tag{S49}$$

and we find that corrections to this term are suppressed exponentially,

$$\int_0^{\hbar\omega_c} \frac{d\zeta}{\zeta} \frac{\sinh^4(\zeta/(2k_BT))}{\sinh^3(\zeta/(k_BT))} \sim \exp\left(-\frac{\hbar\omega_c}{k_BT_c}\right). \tag{S50}$$

Hence, for the determination of the critical temperature, we can neglect the deviation from particle-hole symmetry, and evaluate Eq. (S46) with $f_{\vec{p}'} + f_{-\vec{p}'} - 1 \simeq -\tanh(\zeta/(2k_BT))$. The critical temperature is then connected to the largest eigenvalue of the linearised gap equation by [5]

$$k_BT_c = 1.13\hbar\omega_c e^{-1/\nu}, \tag{S51}$$

where ν is a solution of the eigenvalue equation (5) of the main text. Using $A = 5\times10^{-5}$ and $\omega_c = \omega_0$, we obtain $T_c = 2$ K. For $A = 10^{-5}$, this would even increase to $T_c = 68$ K (However, in this case the eigenvalues grow to order of unity, $\nu \sim 1$, and our weak-coupling approach may no longer be adequate). This approximation cannot account for a finite range of photon momenta in the cavity. So we compare these results in the following with an alternative calculation in section IV D.

D. Check: long-range approximation

Here, we consider the full gap equation for s-wave pairing symmetry. The p-wave case could be treated analogously, but here we are only interested in an estimate for the critical temperature.

At finite temperature, the gap equation is given by

$$\Delta^{(\vec{Q})}(\vec{p}) = \sum_{\vec{p}'} \frac{V^{(\vec{Q})}_{\vec{p},\vec{p}'}}{2N} \frac{\Delta^{(\vec{Q})}(\vec{p}')}{\sqrt{\zeta^2_{\vec{p}'} + |\Delta^{(\vec{Q})}(\vec{p}')|^2}} \left(f_{\vec{p}'} + f_{-\vec{p}'} - 1\right). \tag{S52}$$

In the thermodynamic limit, we obtain Eq. (S46). To solve this integral equation analytically, we note that $c/(a\omega_0) \sim 10^4$ in the THz regime, so the interaction $V_{\vec{p},\vec{p}'}$ decays very quickly in k-space (*i.e.* it is long-range in real space). Thus, only a very short range of wavevectors will be affected, and we can write approximately,

$$\frac{1}{(\omega_0/c)^2 + \left|\vec{p}' - \vec{p}\right|^2} \simeq a_0 \delta(\vec{p}' - \vec{p}), \tag{S53}$$

where a_0 is chosen such that the both sides of Eq. (S53) integrated over the first Brillouin zone yield the same result, *i.e.*

$$a_0 = \int_{BZ} d^2q \, \frac{1}{(\omega_0/c)^2 + \left|\vec{q}\right|^2} \tag{S54}$$

$$\simeq 2\pi \int_0^{q_{\max}} dq \, \frac{q}{(\omega_0/c)^2 + q^2}, \tag{S55}$$

where we introduced a momentum cutoff $q_{\max}$ for the in-plane photon momenta supported by the cavity in the second line which we discuss below. We then obtain

$$a_0 = \pi \log\left[1 + \left(\frac{c}{\omega_0} q_{\max}\right)^2\right]. \tag{S56}$$

The factor 2π in Eq. (S55) stems from the integration over the azimuthal angle. The momentum cutoff $q_{\max}$ evidently depends on the cavity geometry. Our present model of two infinite cavity walls sustains arbitrary q-values, and we can set $q_{\max} = \pi/a$. In this case, we obtain $\log(1 + (\pi c/(a\omega_0))^2) \simeq 20$ (for the values in GaAs). In practice, however, only a finite range of photon momenta will be sustained. To estimate a lower bound for these, we note that the *minimal* photon momentum in a cavity of length L in the x/y-plane should be $q_{\min} = \pi/L$. In [4], this length is $L = 45\ \mu$m, yielding $q_{\min} a = 3.3 \times 10^{-5}$, and thus $\log[\ldots] \geq \log(1 + (1/3)^2) = 0.1$. In [6], the cavity length is given by $L = 2\ \mu$m, thus $q_{\min} = 8.7 \times 10^{-4}$, and $\log[\ldots] \geq 2.9$. In the following, we assume the logarithm to be on the order of unity,

$$a_0 \simeq \pi \tag{S57}$$

The approximation (S53) turns Eq. (S46) into a simple inversion problem, and we obtain at zero temperature

$$\Delta^{(\vec{Q})}_0(\vec{p}) = \sqrt{\left(\frac{\pi V_0 \sum_{i=x,y} (\cos 2p_i a - \cos 2Q_i a)}{4(2\pi)^2}\right)^2 - \zeta^2_{\vec{p}}}, \tag{S58}$$

for $|\zeta_{\vec{p}}| < \pi V_0(\cos 2p_i a - \cos 2Q_i a)/(4(2\pi)^2)$, and zero otherwise, and the critical temperature

$$k_B T_c \simeq \frac{\Delta^{(\vec{Q})}_0}{2}, \tag{S59}$$

where $\Delta^{(\vec{Q})}_0$ is given by Eq. (S58) evaluated at the Fermi surface. For typical values in GaAs heterostructures and using a cavity compression $V \sim \lambda^3/(2 \times 10^4)$, we obtain $V_0 \sim 10^{-3} t$, and the critical temperature

$$T_c \simeq 2 \times 10^{-4} \frac{K}{A}. \tag{S60}$$

Thus, the cavity-mediated interaction can give rise to superconducting condensation in the milliKelvin regime for a wavelength-limited cavity. This temperature is already orders of magnitude larger than those predicted for the free space interaction. The additional enhancement of the vacuum field in nanocavities then pushes the critical temperature into an experimentally accessible regime. For $A = 2 \times 10^{-4}$, we thus obtain $T_c \sim 1$ K, and for $A = 10^{-5}$, $T_c \sim 20$ K. This is roughly in agreement with the previous estimation in section IV C.

V. QUASIPARTICLE HAMILTONIAN

To determine the energy dispersion, we diagonalize the Hamiltonian [10]

$$H_{\mathrm{MF}} = \begin{pmatrix} \epsilon_{\vec{k}} & \Delta^{(\vec{Q}_1)}_{\vec{k}} & \Delta^{(-\vec{Q}_1)}_{\vec{k}} & \Delta^{(\vec{Q}_2)}_{\vec{k}} & \Delta^{(-\vec{Q}_2)}_{\vec{k}} \\ \Delta^{(\vec{Q}_1)*}_{\vec{k}} & -\epsilon_{2\vec{Q}_1 - \vec{k}} & 0 & 0 & 0 \\ \Delta^{(-\vec{Q}_1)*}_{\vec{k}} & 0 & -\epsilon_{-2\vec{Q}_1 - \vec{k}} & 0 & 0 \\ \Delta^{(\vec{Q}_2)*}_{\vec{k}} & 0 & 0 & -\epsilon_{2\vec{Q}_2 - \vec{k}} & 0 \\ \Delta^{(-\vec{Q}_2)*}_{\vec{k}} & 0 & 0 & 0 & -\epsilon_{-2\vec{Q}_2 - \vec{k}} \end{pmatrix}, \tag{S61}$$

where we define $\vec{Q}_1 = k_0(1,1)$ and $\vec{Q}_2 = k_0(1,-1)$. The length k_0 is obtained from the requirement $\epsilon_{\vec{Q}} = 0$. This Hamiltonian contains the mean field values $\Delta^{(\vec{Q})}_{\vec{k}}$ at all four nesting vectors. We approximate the mean fields by exponentials

$$\Delta^{(\vec{Q})}_{\vec{k}} = \Delta_0 \exp(-(\vec{k} - \vec{Q})^2/(2\sigma^2)), \tag{S62}$$

where the width σ is estimated from a fit to the leading eigenfunction [see Fig. 1(d) of the main text] at the given electron density, but the results do not depend sensitively on this width. Furthermore, we fix $\Delta_0 = 10^{-3} t$ (corresponding to a critical temperature in the low-Kelvin regime).

VI. HEXAGONAL LATTICE

The results for a square lattice can be generalised to an arbitrary lattice by writing the electron Hamiltonian as,

$$H_0 = -2 \sum_{\vec{k},\sigma} \sum_{\vec{\delta}} t_{\vec{\delta}} \cos(\vec{k} \cdot \vec{\delta}) c^\dagger_{\vec{k},\sigma} c_{\vec{k},\sigma}, \tag{S63}$$

where the summation over δ runs over nearest-neighbour vectors (for instance, for the square lattice, we simply have $\vec{\delta}_1 = a(1,0)^T$, and $\vec{\delta}_2 = a(0,1)^T$), and t_δ denotes the hopping amplitude along the direction δ. For the case of a hexagonal lattice, we have

$$\vec{\delta}_1 = a\begin{pmatrix}1\\0\end{pmatrix},$$
$$\vec{\delta}_2 = \frac{a}{2}\begin{pmatrix}1\\\sqrt{3}\end{pmatrix}$$
$$\vec{\delta}_3 = \frac{a}{2}\begin{pmatrix}1\\-\sqrt{3}\end{pmatrix}.$$

Similarly, the interaction Hamiltonian reads

$$H_{\text{int}} = \frac{2e}{\hbar}\sum_{\vec{k},\vec{q}}\sum_{\sigma,s}\sum_{\vec{\delta}} t_{\vec{\delta}}\,\vec{\delta}\cdot\hat{e}_{\vec{q},s}\sin\left((\vec{k}+\vec{q}/2)\cdot\vec{\delta}\right) \times\left(a_{\vec{q},s}+a^\dagger_{-\vec{q},s}\right)c^\dagger_{\vec{k}+\vec{q},\sigma}c_{\vec{k},\sigma}. \tag{S64}$$

Repeating the calculations outlined in the manuscript, and assuming for simplicity $t_{\vec{\delta}} = t$ for all $\vec{\delta}$, we can straightforwardly derive the effective interaction

$$V^{(\vec{Q})}_{\vec{p},\vec{p}'} = \frac{V_0}{2}\sum_{\vec{\delta}}\left|\vec{\delta}\right|^2\frac{\cos((\vec{p}+\vec{p}')\cdot\vec{\delta})-\cos(2\vec{Q}\cdot\vec{\delta})}{1+(a\omega_0/c)^2(\vec{p}-\vec{p}')^2}. \tag{S65}$$

The resulting pairing state can be examined with the gap equation (5) of the main text analogously to the square lattice.

The results are shown in Fig. 1, where we consider an electron gas in a hexagonal lattice with otherwise the same parameters as a gas in a GaAs heterostructure, *i.e.* relative permittivity $\epsilon = 13$, electron band mass $m^* = 0.069m_e$, chemical potential $\mu = -3.98t$, lattice constant $a = 5.6$ Å, and a cavity frequency $\omega_0 = 2\pi\times 5$ THz. The cavity compression is chosen as $A = 10^{-4}$. [1]

Fig. 1(a) shows the coupling strength in reciprocal space. The gray vectors indicate linearly independent nesting vectors $\vec{Q}$. Panels (b) and (c) then show the dominating eigenvalues of Eq. (5), and the eigenfunctions, respectively. Just like in the square lattice, the first two eigenvalues correspond to a singlet and a triplet order, respectively. The main influence of the lattice consists in changing the nesting vectors, thus giving rise to a distinct pair density structure.

VII. INFLUENCE OF WEAK DISORDER

To assess the impact of small energetic disorder on the Amperean pairing, we write the energy dispersion as

$$\epsilon_{\vec{k}} = -2t(\cos(k_x a)+\cos(k_y a)) - \mu + \epsilon_{\text{disorder}}(\vec{k}), \tag{S66}$$

where the final term $\epsilon_{\text{disorder}}(\vec{k})$ represents a weak disorder potential. In the following simulations, it is created from the interpolation of random values drawn from a Gaussian distribution with zero mean, *i.e.* $\langle\epsilon_{\text{disorder}}(\vec{k})\rangle = 0$ (where $\langle\ldots\rangle$ denotes the ensemble average), and variance $\langle\epsilon^2_{\text{disorder}}(\vec{k})\rangle = 10^{-4}t$.

The disorder is expected to have two consequences. First, it slightly changes the Fermi surface. Second, it affects the density of states at the Fermi surface, and thus the number of electrons locally available for pairing. The impact on the leading eigenvalue of the linearised gap equation, and hence on the critical temperature, is investigated in Fig. 2, where the eigenvalues are plotted for different disorder realisations. It appears that on average the weak disorder has a (very weak) positive effect on the eigenvalue. This can be understood as a consequence of the long-range nature of the cavity-mediated interaction. The disorder can locally enhance the density of states in reciprocal space, and since only electrons with closely neighbouring k-values can pair effectively, this local enhancement can outweigh the reduction elsewhere in k-space. It should be noted, however, that our simple approach cannot take the reduction of the electronic coherence length into account, which could counteract this weak enhancement.

[1] K. Kakazu and Y. S. Kim, Phys. Rev. A **50**, 1830–1839 (1994).
[2] Y. Todorov, Phys. Rev. B **91**, 125409 (2015).
[3] D. Hagenmüller, S. De Liberato and C. Ciuti, Phys. Rev. B **81**, 235303 (2010).
[4] C. Maissen et al., Phys. Rev. B **90**, 205309 (2014).
[5] V. P. Mineev and M. Sigrist, 129–154 in: Non-Centrosymmetric Superconductors: Introduction and Overview (Springer, Berlin Germany 2012).
[6] X. Gan et al., Nano Lett. **12**, 5626 (2012).
[7] Q. Zhang et al., Nature Phys. (2016).
[8] G. Scalari et al., Science **335**, 1323 (2012).
[9] O. Cotlet, S. Zeytinoglu, M. Sigrist, E. Demler and A. Imamoglu, Phys. Rev. B **93**, 054510 (2016).
[10] P. A. Lee, Phys. Rev. X **4**, 031017 (2014).

[1] Please note that this theoretical model has a much larger electron density than the square lattice model for GaAs heterostructures in the main text which is why a smaller cavity compression is sufficient to realise pairing with observable critical temperatures. In practice, a larger electron density should result in a larger electron band mass, and hence a reduced hopping amplitude t.

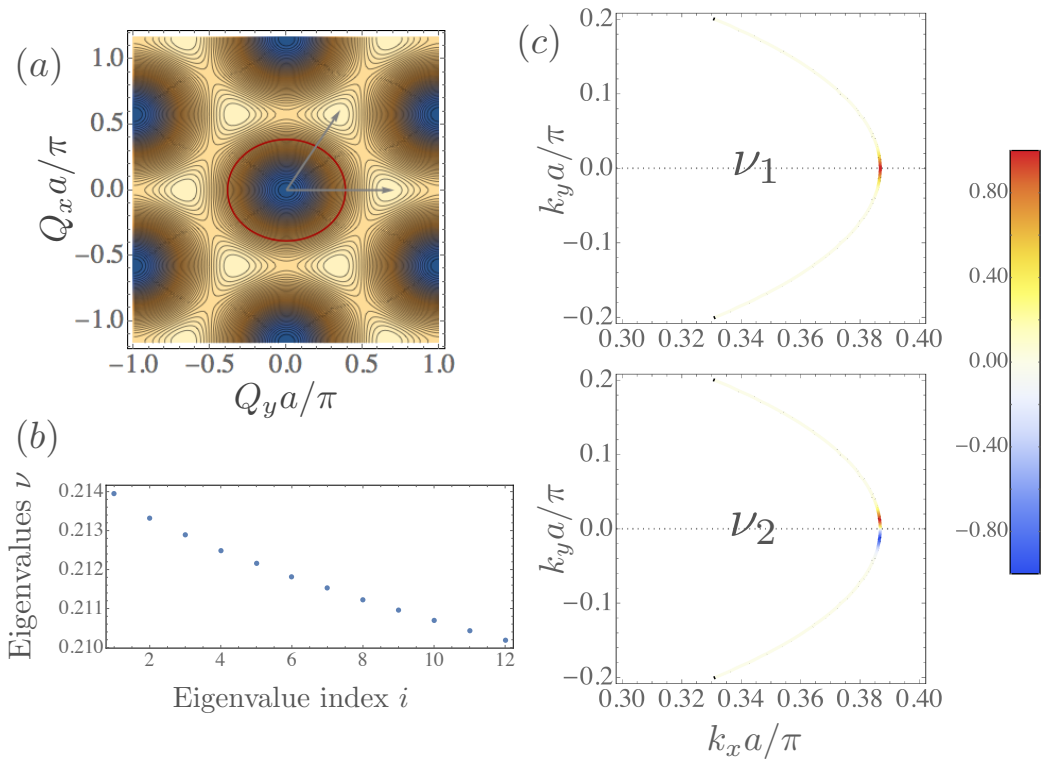

Supplementary Information, Figure 1. (a) Contour plot of the numerator of Eq. (S65) at $\vec{p} = \vec{p}' = 0$. The solid red line indicates the Fermi surface at $\mu = -3.98t$, and the gray vectors point towards the maximal Q-vectors $\pi(1/\sqrt{2}, 0)$ and $\pi(1, \sqrt{3})/2^{3/2}$. (b) Eigenvalues of the linearised gap equation (5) of the main text. We used the values for GaAs, as in Fig. 1 of the main text. (c) The eigenfunctions pertaining to the two largest eigenvalues of panel (b).

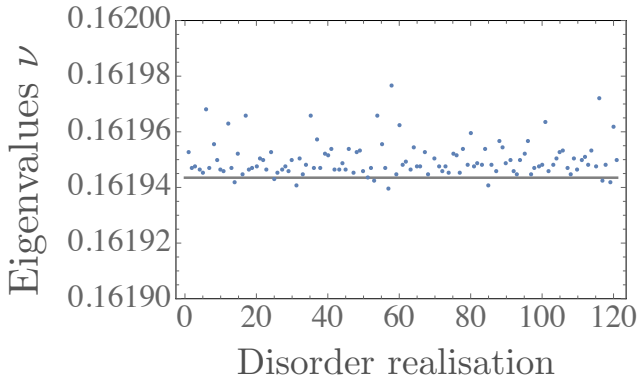

Supplementary Information, Figure 2. Variation of the leading eigenvalues of the linearised gap equation (5) for different disorder realisations according to Eq. (S66). The solid gray line indicates the value obtained without disorder.